

Finite element models for the study of hydrogen embrittlement of steel structures

Daniella LOPES PINTO ^{1,2*}

daniella.lopes_pinto@minesparis.psl.eu

Thesis director: Jacques BESSON ¹

Industrial advisor: Nikolay OSIPOV ²

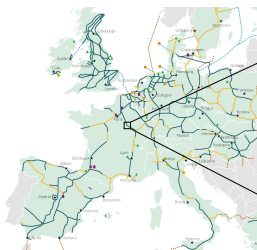
¹ Centre des Matériaux, Mines Paris

² Transvalor S.A.

Thesis defense

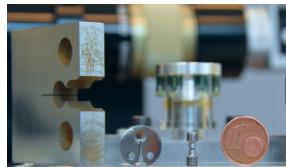
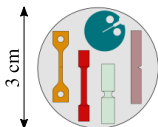
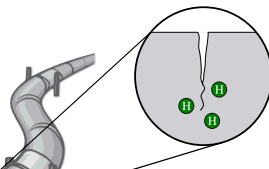
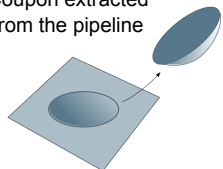
March 7th 2025

- ▶ In the context of **energy transition**, **hydrogen** plays an important role as an **energy vector**
- ▶ Hydrogen can be produced from other **renewable sources**, such as wind and solar
- ▶ Hydrogen transport using **existing natural gas pipelines** (40,000 km in France, €50 billion in assets, up to 80 years old) is a proposal for hydrogen transport

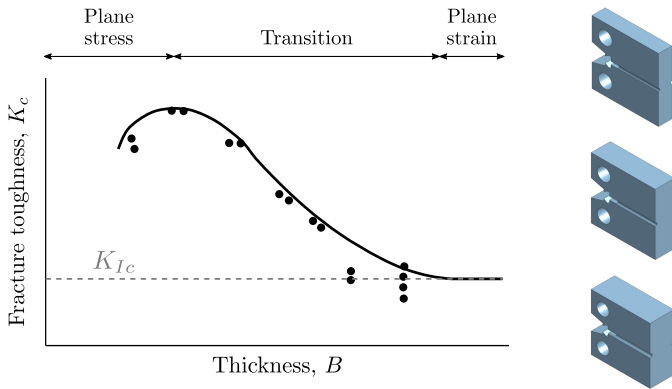


- ▶ The steels used in gas pipelines are typically susceptible to **hydrogen embrittlement**
- ▶ Hydrogen embrittlement: ductility and toughness reduction, premature failure
- ▶ Measure material properties from **small samples** without service interruption

Coupon extracted
from the pipeline



- ▶ Transferability from sub-size specimens to a full scale structure → **Specimen size significantly influences toughness**
- ▶ Beyond a critical thickness, toughness becomes relatively insensitive to further increases



Adapted from Barsom and Rolfe, 1987.

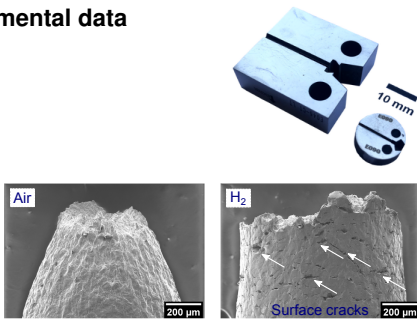
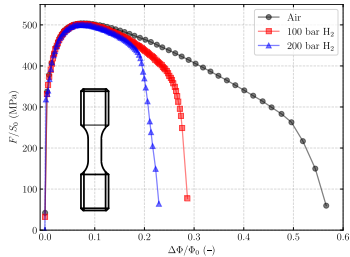
► Hydrogen embrittlement:

- ▶ Develop a model coupling plasticity, damage, and hydrogen diffusion
- ▶ Reproduce the degradation of the materials mechanical properties, ductility and toughness loss, multi-crack initiation

► Fracture toughness simulations:

- ▶ Analyze the effect of the specimen's size and thickness on fracture toughness through numerical simulations

► Validate the model against experimental data



Introduction

Hydrogen inside metals

Finite element formulation

Numerical simulations

Pressurized disks tests

Hydrogen embrittlement modeling

Simulation of fracture toughness tests

Conclusions and perspectives

Introduction

Hydrogen inside metals

Finite element formulation

Numerical simulations

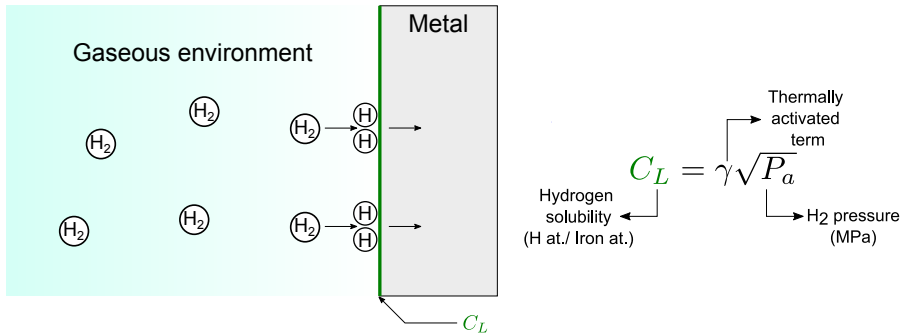
Pressurized disks tests

Hydrogen embrittlement modeling

Simulation of fracture toughness tests

Conclusions and perspectives

- ▶ **Sieverts' law:** The solubility of a diatomic gas in a metal is proportional to the square root of the gas pressure

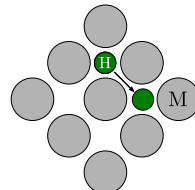


- Model from Sofronis and McMeeking (1989) and corrected by Krom *et al.* (1999)

- **Hydrogen concentration:** $C = C_L + C_T$

- Lattice concentration: $C_L = \beta N_L \theta_L$

- Trapped concentration: $C_T = \sum_i^N C_T^i = N_T^i(\kappa) \theta_T^i$



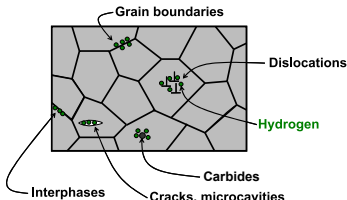
- **Hydrogen flux:**

$$J = -D_L \nabla C_L + \frac{D_L C_L V_H}{RT} \nabla p$$

- **Oriani's instantaneous equilibrium:**

$$\frac{1 - \theta_L}{\theta_L} \frac{\theta_T^i}{1 - \theta_T^i} = \exp \left(\frac{W_B^i}{RT} \right)$$

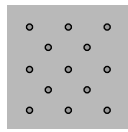
(Coupling terms)



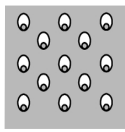
- The **ductile behavior** of the metal is described by the well-known **GTN model** (Tvergaard *et al.* 1984):

$$\frac{\sigma_{eq}^2}{\sigma_F^2} + 2q_1 f_* \cosh\left(\frac{q_2}{2} \frac{\sigma_{ii}}{\sigma_F}\right) - 1 - q_1^2 f_*^2 = 0 \quad \text{where } f^* = \text{function}(f)$$

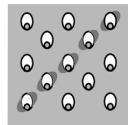
$$\dot{f} = \dot{f}_{nucleation} + \dot{f}_{growth}$$



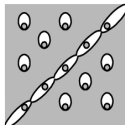
Impurities or second phase particles



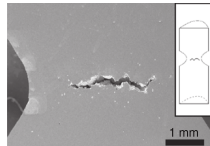
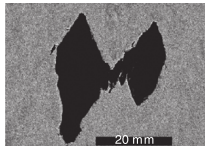
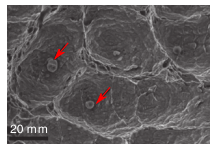
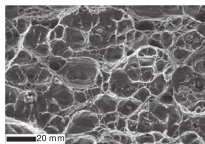
Void nucleation and growth



Strain localization



Void coalescence and fracture

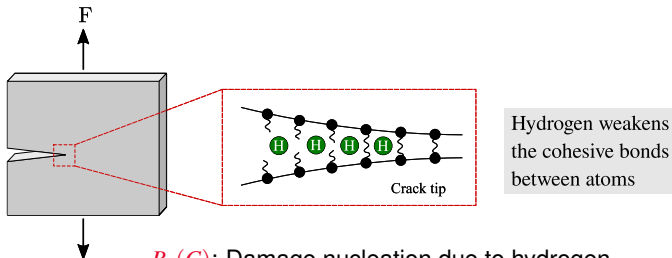


- **Void growth:** Unchanged due to mass conservation

$$\dot{f}_g = (1 - f_g) \text{trace}(\dot{\varepsilon}_p)$$

- **Void nucleation:** Proposed dependence on hydrogen concentration

$$\dot{f}_n = A_n(\kappa)\dot{\kappa} + B_n(C)\dot{\kappa} \quad (\text{Coupling terms})$$



Hydrogen weakens
the cohesive bonds
between atoms

$B_n(C)$: Damage nucleation due to hydrogen
HEDE (Hydrogen Enhanced Decohesion)

Introduction

Hydrogen inside metals

Finite element formulation

Numerical simulations

Pressurized disks tests

Hydrogen embrittlement modeling

Simulation of fracture toughness tests

Conclusions and perspectives

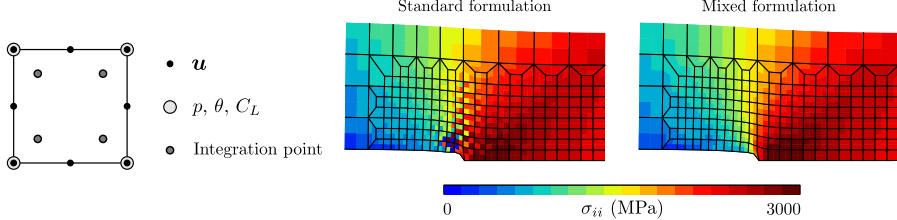
- ▶ Fully implicit finite strain framework
- ▶ Based on a mixed formulation: u, p, θ (Zhang *et al.* 2017) and C_L
- ▶ Quadratic elements with reduced integration
- ▶ **Aim:** better pressure fields by avoiding volumetric locking



Advantage

∇p can be directly computed from nodal values

$$J = -D_L \nabla C_L + \frac{D_L C_L V_H}{RT} \nabla p$$



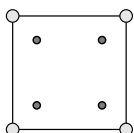
- ▶ The use of **quadratic elements** with additional dofs can be very **time consuming**

- ▶ **B -bar** (or \bar{B}) formulation (Hughes, 1980):

- ▶ Linear elements with full integration
- ▶ Solves volumetric locking by modifying the strain-displacement matrix:

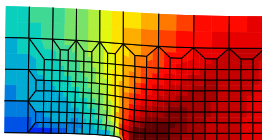
$$\bar{\mathbf{B}} = \mathbf{B}_d + \bar{\mathbf{B}}_h$$

- ▶ To avoid extrapolating p to the nodes for ∇p computation, it is considered as a dof



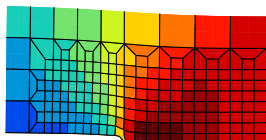
- \mathbf{u}, p, C_L
- Integration point

Mixed formulation

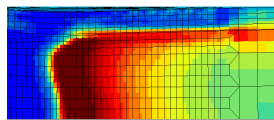
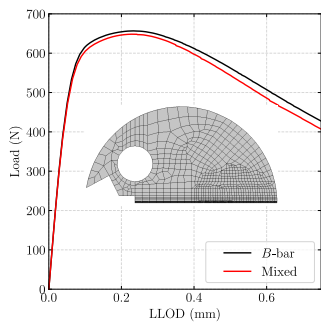


0 σ_{ii} (MPa) 3000

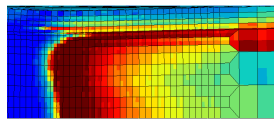
B -bar formulation



- ▶ Test on a Disk Compact Tension (DCT) specimen with 5200 elements:
 - ▶ **Mixed formulation:** 103,762 dofs, 1h 40 minutes to complete
 - ▶ **B-bar formulation:** 33,974 dofs, 18 minutes to complete
- ▶ Slightly higher force for the **B-bar** formulation → Linear elements are inherently stiffer since they have less nodes



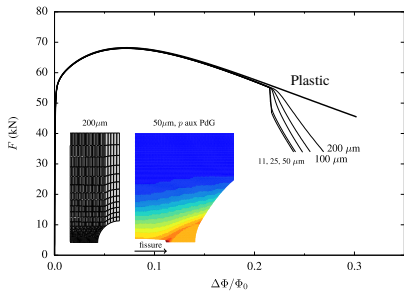
Mixed formulation



B-bar formulation

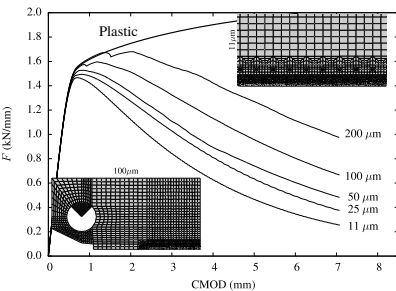
0 σ_{ii} (MPa) 2000

- ▶ Damage models such as the GTN model are known to induce **spurious mesh dependency** (element size, type and orientation)
- ▶ To solve this problem, it is proposed to use a **nonlocal damage model** based on the **implicit gradient** by Peerlings *et al.*, 1996



Notched tensile (NT) specimen

(Besson, 2021)

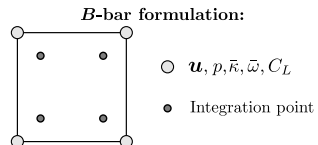
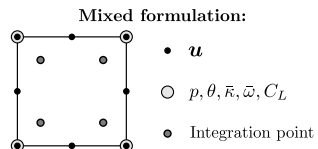
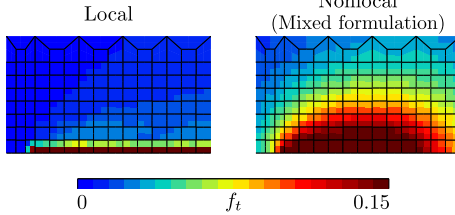


Compact tension (CT) specimen

- ▶ Two variables are used (two associated internal lengths: $\bar{\omega}$ and $\bar{\kappa}$):
- ▶ **Plastic volume variation:** $\dot{\bar{\omega}} - \ell_{\omega}^2 \Delta \bar{\omega} = \omega$ where $\omega = \text{trace}(\dot{\varepsilon}_p)$
- ▶ **Accumulated plastic strain:** $\dot{\bar{\kappa}} - \ell_{\kappa}^2 \Delta \bar{\kappa} = \kappa$
- ▶ The modified evolution laws for the damage variables are now:

▶ **Void growth:** $\dot{f}_g = (1 - f_g) \dot{\bar{\omega}}$

▶ **Void nucleation:** $\dot{f}_n = A_n \dot{\bar{\kappa}} + B_n(C) \dot{\bar{\kappa}}$



Introduction

Hydrogen inside metals

Finite element formulation

Numerical simulations

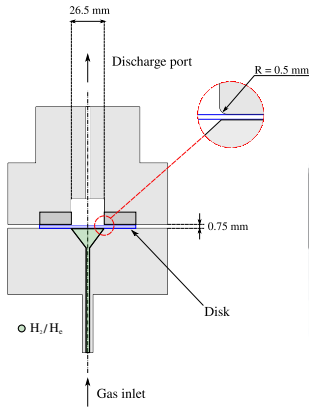
Pressurized disks tests

Hydrogen embrittlement modeling

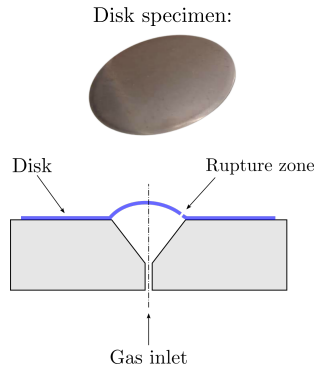
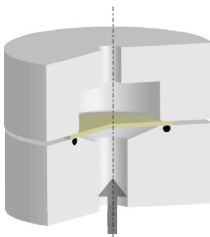
Simulation of fracture toughness tests

Conclusions and perspectives

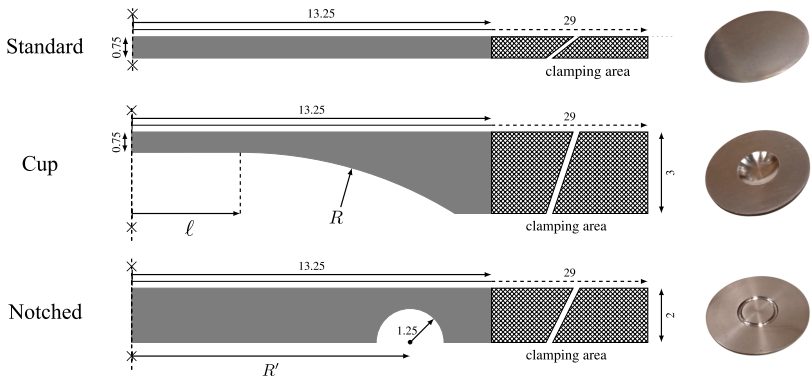
- ▶ **ISO 11114-4 standard:** uses pressurized disk tests for selecting metallic materials resistant to hydrogen embrittlement
- ▶ Disk often fails in the clamping zone
- ▶ **First step:** redesigning the disk geometry to control failure location



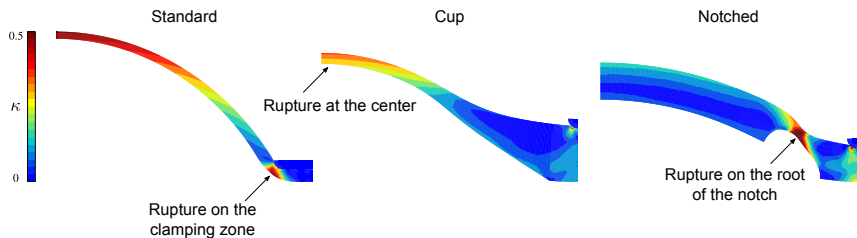
$$\text{HEI} = \frac{P_r(\text{He})}{P_r(\text{H}_2)}$$



- ▶ New proposed geometries:
 - ▶ No need to modify the test setup
 - ▶ Keep the same minimum thickness of the standard (0.75 mm)
- ▶ Optimization with respect to ℓ , R and R' with FE simulations considering an elasto-plastic behavior



- ▶ The location of the maximum accumulated plastic strain (κ) corresponds to the failure location



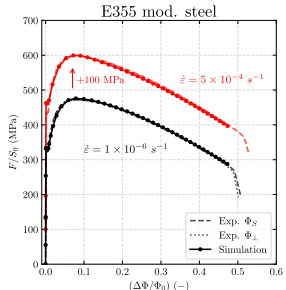
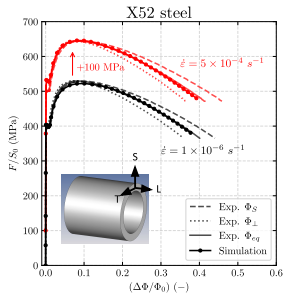
► X52 vintage steel:

- ▶ Yield strength: 400 MPa
- ▶ Different elongation at rupture in T and L directions

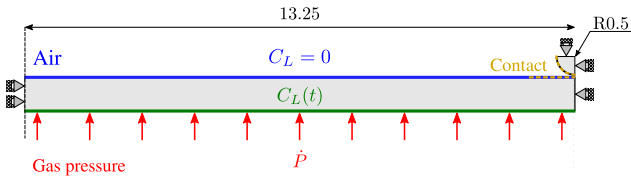
► E355 mod. steel:

- ▶ Yield strength: 330 MPa
 - ▶ Higher elongation at rupture and lower Ultimate Tensile Strength in relation with the vintage material
 - ▶ Similar elongation at rupture in both directions
- Elasto(visco)-plastic model coefficients' identified through optimization:

$$\sigma_F(p) = \max(\sigma_L, \sigma_0 + Q_1(1 - \exp(-b_1 p)) + Q_2(1 - \exp(-b_2 p)) + H p)$$

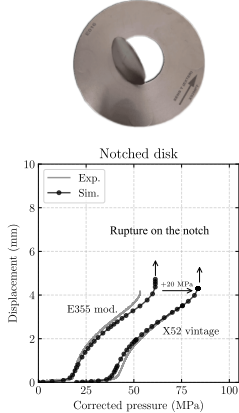
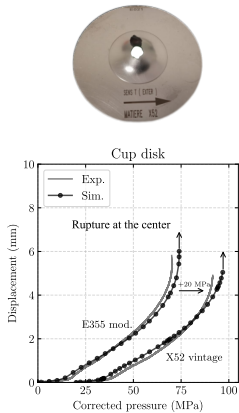
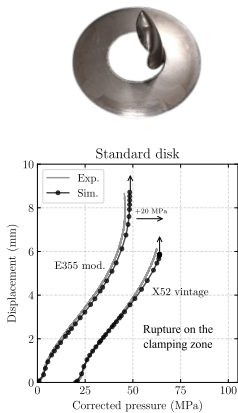
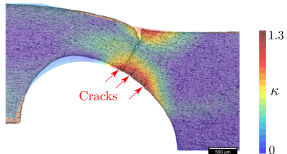


- ▶ Axisymmetric model, quadratic elements with reduced integration (mixed formulation)
- ▶ Hydrogen diffusion parameters taken from the literature
- ▶ Since damage is not considered into the numerical model, the simulations were stopped once they reached experimentally observed rupture pressure (P_r)
- ▶ Model's boundary conditions:



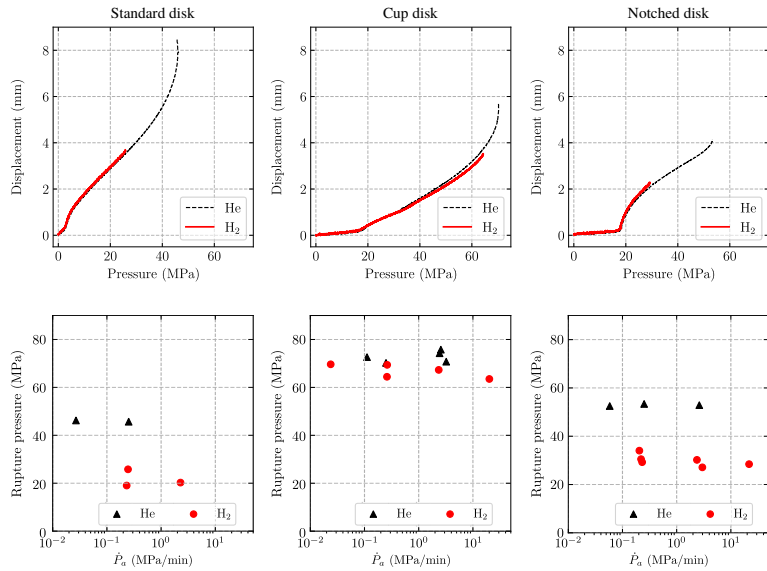
Results under helium

- ▶ Successfully modification of fracture location
- ▶ Failure is primarily driven by plasticity and occurs under a limit load scenario



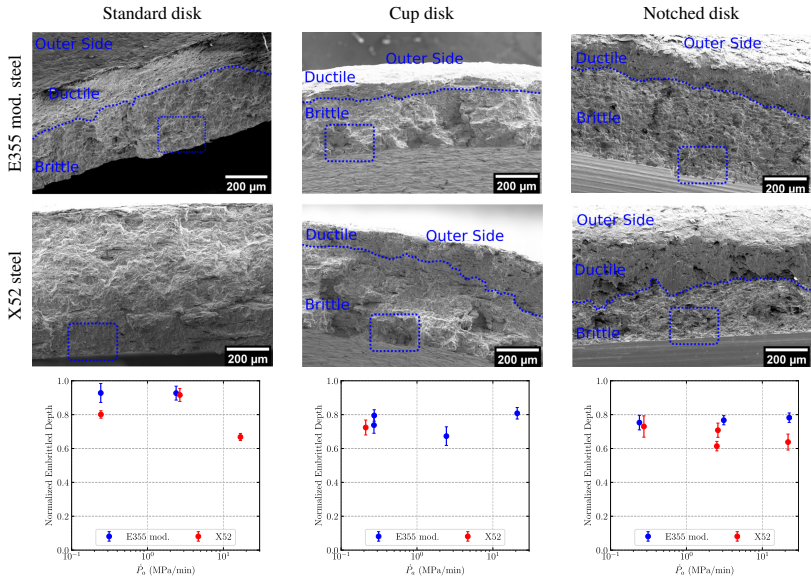
(Experimental data: Santana *et al.*, 2024)

Results under hydrogen (E355 mod. steel)



(Experimental data: Santana *et al.*, 2024)

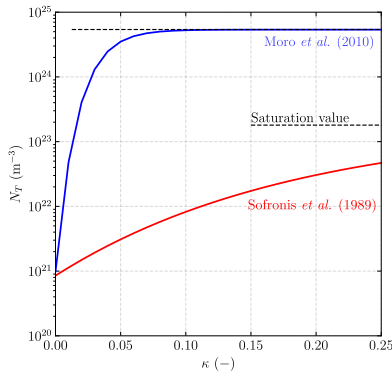
Hydrogen embrittled depth



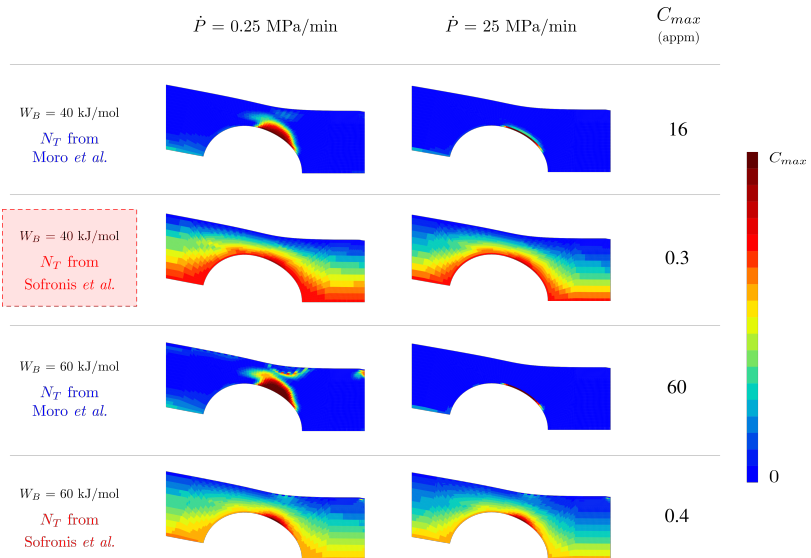
- ▶ Considers only one kind of trap: dislocations
- ▶ Trap binding energies (W_B) and trap densities (N_T) were taken from the literature and analyzed based on the experimental observations
- ▶ Based on the models proposed by Moro *et al.* (2010) and Sofronis *et al.* (1980), four cases emerge

$$W_B = \begin{cases} 40 \text{ kJ/mol} \\ 60 \text{ kJ/mol} \end{cases}$$

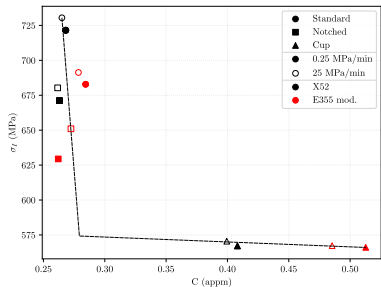
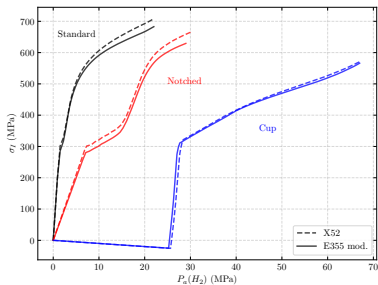
$$N_T = \begin{cases} \log_{10} N_T = 24.73 - 3.74 \exp(-60.17\kappa) \\ \log_{10} N_T = 23.26 - 2.33 \exp(-5.5\kappa) \end{cases}$$



Hydrogen embrittled depth



- ▶ Specimens that develop higher principal stress (σ_I) in the fracture zone fail at a lower hydrogen pressure ($P_a(H_2)$)
- ▶ The total hydrogen concentration reduces the maximum principal stress that triggers fracture



Introduction

Hydrogen inside metals

Finite element formulation

Numerical simulations

Pressurized disks tests

Hydrogen embrittlement modeling

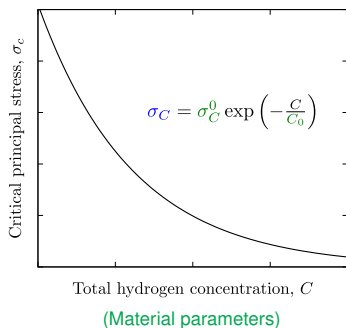
Simulation of fracture toughness tests

Conclusions and perspectives

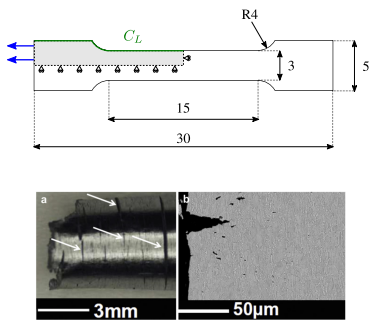
- ▶ **Database:** Briottet *et al.*, 2012 and Moro *et al.*, 2010: *Effect of gaseous hydrogen on the mechanical properties of steel*
- ▶ **Material:** high-strength steel (API X80 grade) in an environment of hydrogen and neutral gas
- ▶ As HE corresponds to **quasi-cleavage**, a **stress dependance** is introduced to the nucleation law
- ▶ The function expressing the nucleation rate due to quasi-cleavage is:

$$B_n(C) = \frac{B_0}{\sigma_C^0} (\sigma_I - (1 - q_1 f_*) \sigma_C)$$

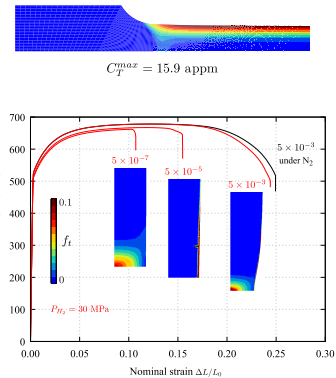
- ▶ Hydrogen decreases the critical stress to trigger void nucleation



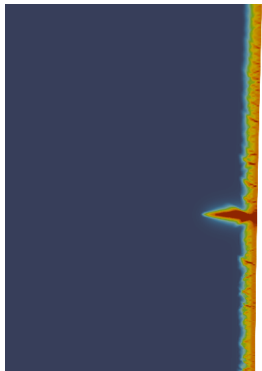
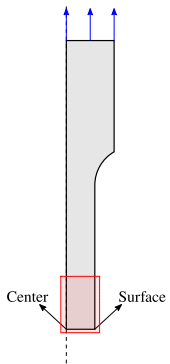
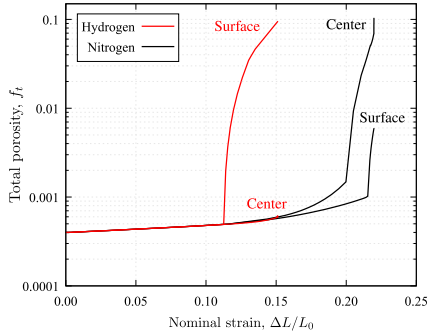
- ▶ Tensile tests under different strain rates under hydrogen gas
- ▶ Slower rates lead to important ductility losses



(Experimental data: Briottet *et al.*, 2012)

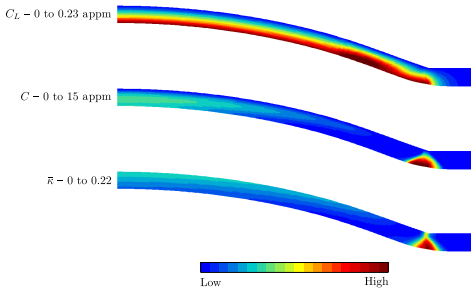
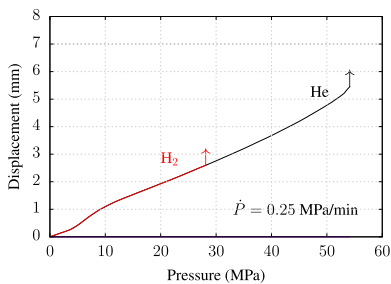
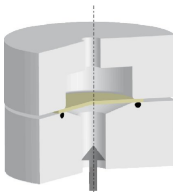


- ▶ Different damage evolution under hydrogen environment
- ▶ Multicrack initiation on the surface



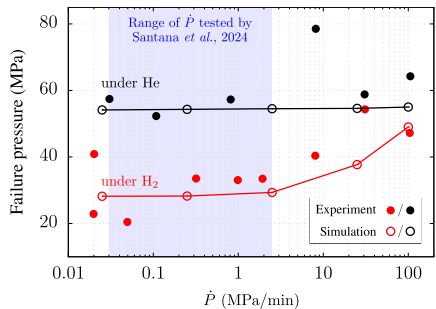
Hydrogen effect:

- ▶ Lower pressure at rupture with decreased ductility
- ▶ Higher hydrogen concentration in the rupture zone

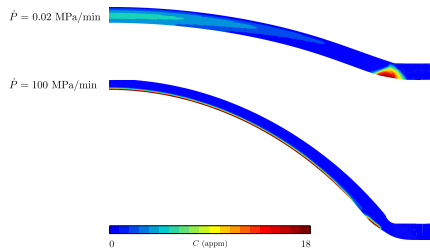


Effect of the pressurization rate:

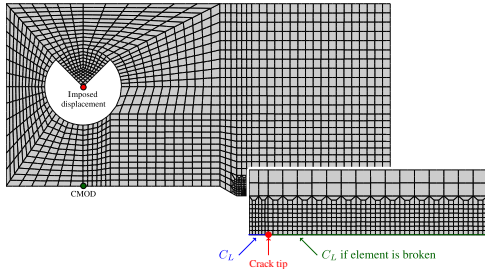
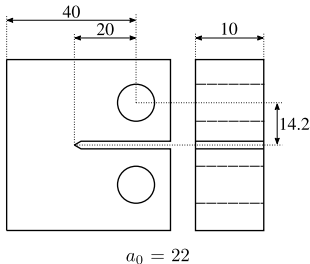
- ▶ Tests under different pressurization rates on H_e and H₂ gases
- ▶ **Lower pressurization rate → Higher embrittlement** since has a longer time to diffuse



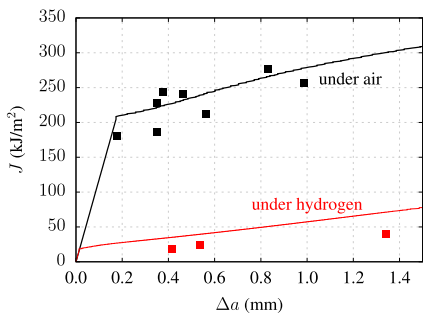
(Experimental data: Briottet *et al.*, 2012)



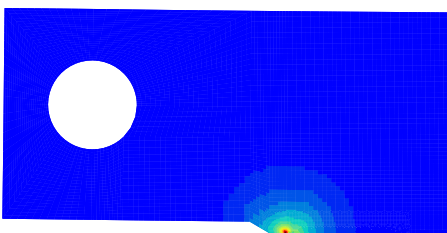
- ▶ 2D Compact Tension (CT) specimen - *plane strain*
- ▶ Uniaxial imposed displacement
- ▶ Environment: air and hydrogen (30 MPa)
- ▶ Lattice concentration (C_L) derived from Sieverts' law imposed on the newly formed crack



- ▶ Crack length: post-processing considering broken elements $f_* = 0.99 \times 1/q_1$
- ▶ J -integral computation: ASTM E1820 standard considering the simulated Load-CMOD curve



Hydrogen diffusion through the crack lips:



Introduction

Hydrogen inside metals

Finite element formulation

Numerical simulations

Pressurized disks tests

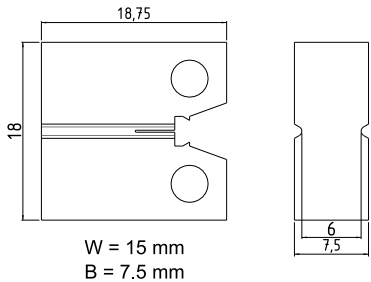
Hydrogen embrittlement modeling

Simulation of fracture toughness tests

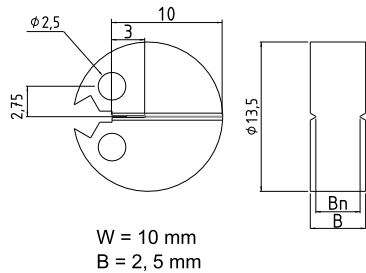
Conclusions and perspectives

- ▶ X52 vintage steel
- ▶ Tube thickness: 7.92 mm
- ▶ Tests using standard and sub-size specimens
- ▶ Pre-cracking and side grooves with $B_n = 10\%B$ at each side
- ▶ Experiments and simulations **without hydrogen**

Standard Compact Tension (CT):

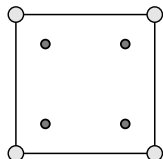


Mini Disk Compact Tension (mDCT):

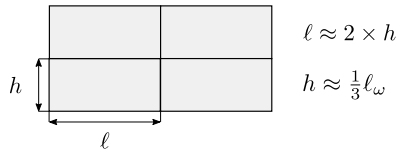


► Nonlocal GTN model with two internal lengths:

- ℓ_κ : accumulated plastic strain (void nucleation)
- ℓ_ω : plastic volume change (void growth)
- Typical element size used in nonlocal models for pipeline steel simulations (Madi et al., 2020): $\ell_\omega = 100 \mu\text{m}$
- The length scale associated with secondary nucleation is likely smaller:
 $\ell_\kappa = 33 \mu\text{m}$



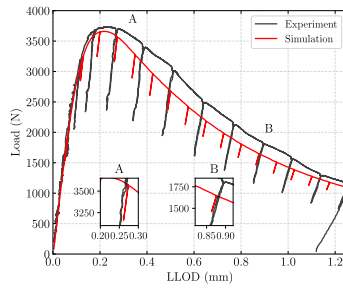
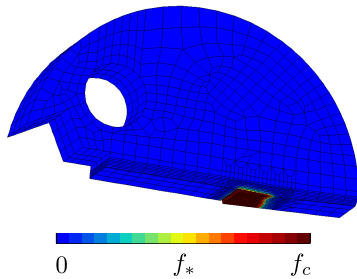
- $\{\mathbf{u}\}, \{\bar{\omega}\}, \{\bar{\kappa}\}$
- Integration point



- ▶ **Element removal technique:** an element of the mesh is removed when a predefined number of its integration points reach a critical porosity value:

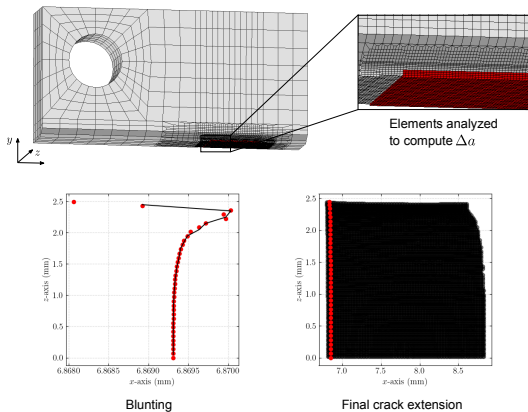
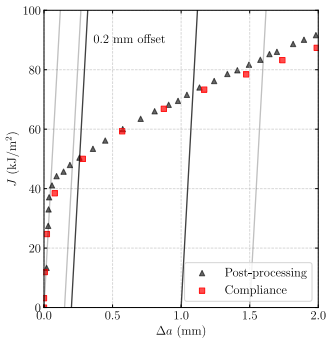
$$f_c = 1/q_1 - \epsilon$$

- ▶ **First method:** compliance technique $\rightarrow \Delta a$ is computed at the same way as in the experiments
 - ▶ **Drawback:** the load, hold, and unload steps into simulations significantly increases computation time



► Second method: Post-processing

- The initial crack front is identified and the porosity values are analyzed on elements in the crack propagation zone
- Elements with integration points reaching the critical porosity value (f_c) are considered broken. The crack front is updated after propagation.



- ▶ The coefficients of the constitutive law were directly identified using the fracture toughness specimens
- ▶ The hardening law is slightly different from the one previously presented → Dispersion observed for the X52 steel
- ▶ Hardening law:

$$\sigma_F(\kappa) = \max(340, 243 + 158(1 - \exp(-28.39\kappa)) + 399(1 - \exp(-269\kappa)))$$

- ▶ Damage coefficients:

$$q_1 = 1.25$$

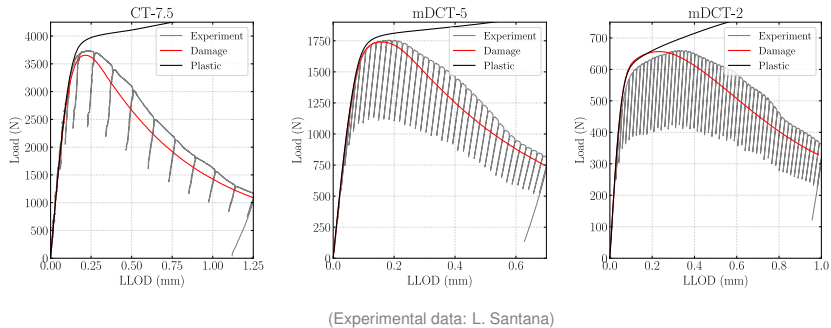
$$q_2 = 1.40$$

$$\dot{f}_n = A_n (\bar{\kappa} > \kappa_c) \dot{\bar{\kappa}} \quad \text{with}$$

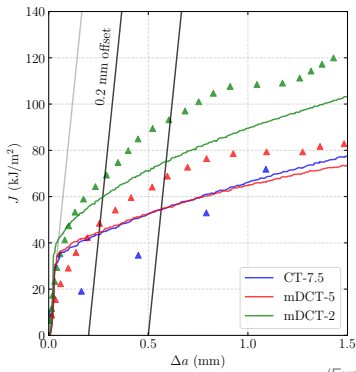
$$A_n = 1.0 \quad \text{and} \quad \kappa_c = 0.15 \rightarrow \textbf{High and early void nucleation}$$

Results: simulations vs. experiments

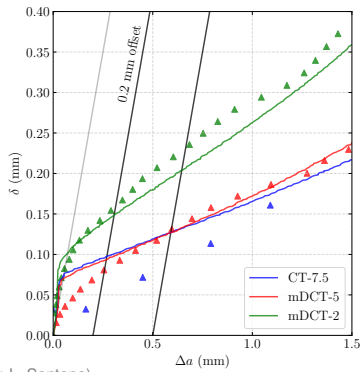
- ▶ Mesh dimensions precisely match the specimen dimensions for each test
- ▶ An elasto-plastic model fails to accurately represent the fracture toughness test once crack propagation begins



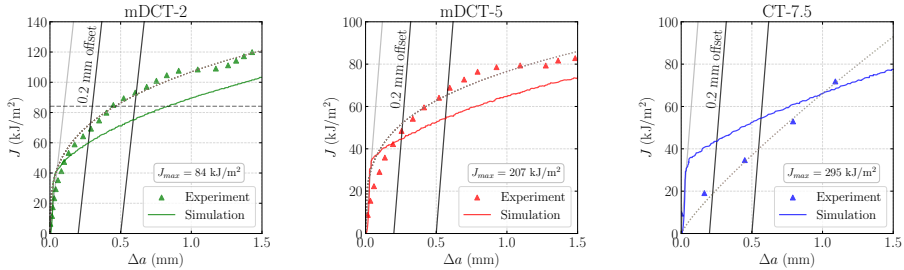
- ▶ Relatively low toughness values
- ▶ Crack propagation initiates later for the simulations → This delay was partially addressed by reducing the void nucleation threshold
- ▶ J and δ (CTOD) values increase as specimen size decreases



(Experimental data: L. Santana)



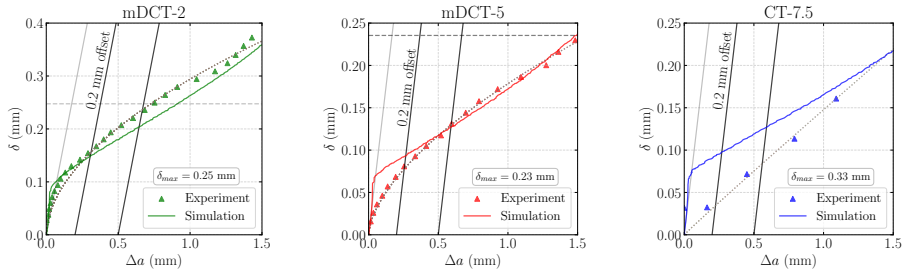
Results: simulations vs. experiments



Specimen	J_{max} (kJ/m ²)	$J_{0.2}$ (kJ/m ²)		$J_{0.5}$ (kJ/m ²)	
		Experiment	Simulation	Experiment	Simulation
mDCT-2	84	73	59	92	76
mDCT-5	207	52	43	65	55
CT-7.5	295	19	40	42	55

Construction line: $J = 2\sigma_0 \Delta a$ (ASTM E1820)

Results: simulations vs. experiments

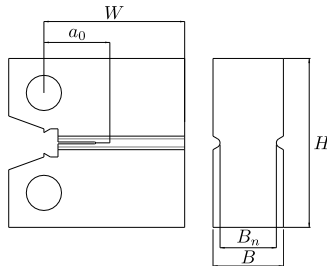


Specimen	δ_{max} (mm)	$\delta_{0.2}$ (mm)		$\delta_{0.5}$ (mm)	
		Experiment	Simulation	Experiment	Simulation
mDCT-2	0.25	0.16	0.12	0.24	0.21
mDCT-5	0.24	0.08	0.08	0.13	0.13
CT-7.5	0.33	0.03	0.08	0.08	0.13

Construction line: $\delta = 1.4\Delta a$ (ASTM E1820)

Homothetic specimens:

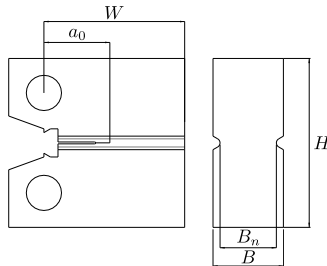
- ▶ **Homothetic CT specimens** → Dimensions scaled systematically from the smallest to the largest
- ▶ $B/W = 0.5$ and $a_0/W = 0.55$ for all cases
- ▶ Each mesh was generated individually, ensuring correct element size with respect to the internal length



	W (mm)	a_0 (mm)	B (mm)	H (mm)
CT-3.125	6.25	3.4375	3.125	7.5
CT-6.25	12.5	6.875	6.25	15
CT-12.5	25	13.75	12.5	30
CT-20	40	22	20	60
CT-25	50	27.5	25	60
CT-50	100	55	50	120

Homothetic specimens:

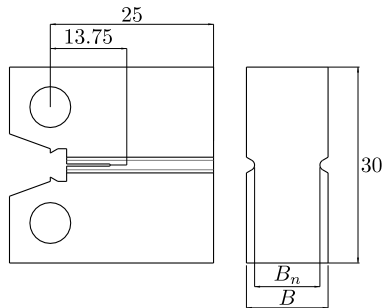
- ▶ **Homothetic CT specimens** → Dimensions scaled systematically from the smallest to the largest
- ▶ $B/W = 0.5$ and $a_0/W = 0.55$ for all cases
- ▶ Each mesh was generated individually, ensuring correct element size with respect to the internal length



	W (mm)	a_0 (mm)	B (mm)	H (mm)
CT-3.125	6.25	3.4375	3.125	7.5
CT-6.25	12.5	6.875	6.25	15
CT-12.5	25	13.75	12.5	30
CT-20	40	22	20	60
CT-25	50	27.5	25	60
CT-50	100	55	50	120

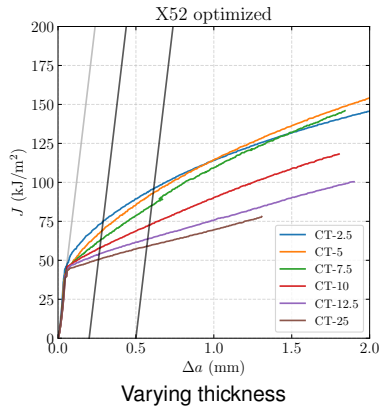
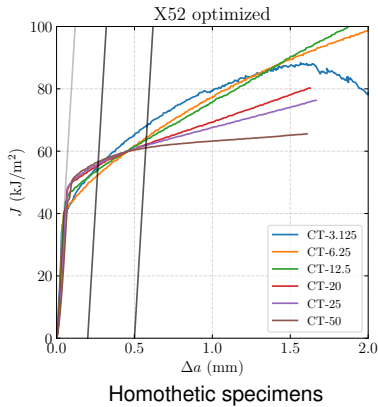
Varying thickness:

- **Varying thickness** → Specimen with the dimensions corresponding to a CT-12.5 with different thickness values

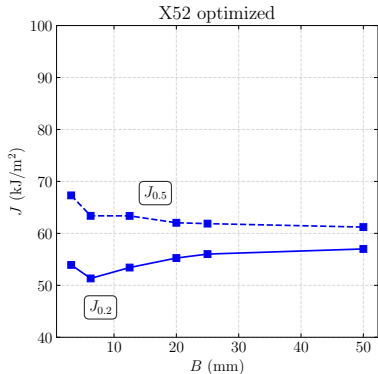
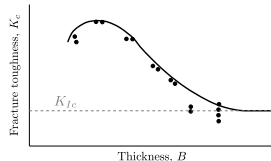


	W (mm)	a_0 (mm)	B (mm)	H (mm)
CT-2.5	25	13.75	2.5	30
CT-5	25	13.75	5	30
CT-7.5	25	13.75	7.5	30
CT-10	25	13.75	10	30
CT-12.5	25	13.75	12.5	30
CT-25	25	13.75	25	30

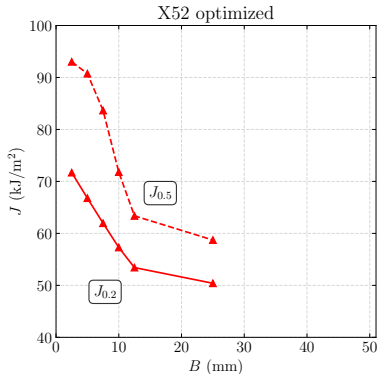
- ▶ Coefficients identified for the X52 steel
- ▶ **Homothetic specimens:** Minor effect on toughness
- ▶ **Varying thickness:** Toughness decreased with thickness



- ▶ Size and thickness effect on $J_{0.2}$ and $J_{0.5}$
- ▶ Fracture toughness and thickness do not have a bijective relationship



Homothetic specimens



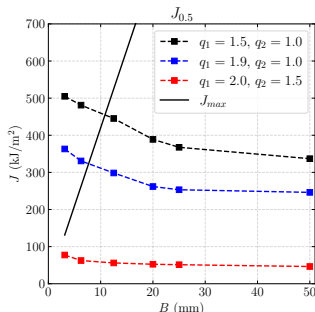
Varying thickness

Varying damage coefficients:

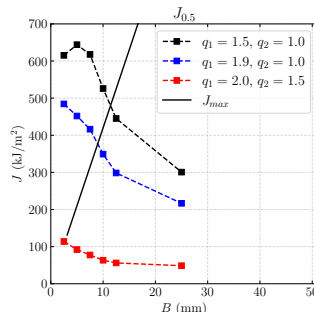
- ▶ **Hardening law:** same as the X52
- ▶ **GTN's coefficients:**
 - ▶ $q_1 = 1.5, q_2 = 1.0 \rightarrow \text{Most ductile case}$
 - ▶ $q_1 = 1.9, q_2 = 1.0$
 - ▶ $q_1 = 2.0, q_2 = 1.5 \rightarrow \text{Less ductile case}$
- ▶ $\uparrow q_1$: increases void growth sensitivity, causing earlier growth and **reduced ductility**
- ▶ $\uparrow q_2$: Leads to early crack initiation, **reduced ductility**, and abrupt fracture
- ▶ **Low void nucleation:** $A_n = 0.2$ and $\kappa_c = 0.8$

Varying damage coefficients:

- ▶ Homothetic specimens exhibit more stable toughness values
- ▶ More ductile material present more size effects
- ▶ Even tests considered valid according to the standard can still display size effects
- ▶ No bijective relationship between toughness and thickness



Homothetic specimens



Varying thickness

Introduction

Hydrogen inside metals

Finite element formulation

Numerical simulations

Pressurized disks tests

Hydrogen embrittlement modeling

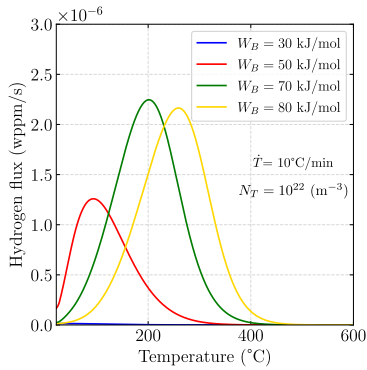
Simulation of fracture toughness tests

Conclusions and perspectives

- ▶ **Comprehensive HE modeling:** Developed a numerical framework integrating hydrogen diffusion, plasticity, and damage mechanisms.
- ▶ **Modified nonlocal GTN model:** Incorporated hydrogen-enhanced decohesion (HEDE) and diffusion effects, accelerating damage evolution and leading to premature failure.
- ▶ **Experimental validation & trends:** Applied the model to pressurized disk, tensile, and fracture toughness tests, accurately capturing key experimental trends such as toughness and ductility loss, strain rate effects, and the transition from ductile to quasi-brittle failure.
- ▶ **Fracture toughness & size effects:** Investigated the influence of specimen size and thickness on fracture toughness across different material configurations.
- ▶ **Key contributions:** Provided a comprehensive framework for HE simulation, improving understanding of hydrogen-induced damage in pipeline steels.

► Thermal Desorption Spectroscopy (TDS) simulations and tests:

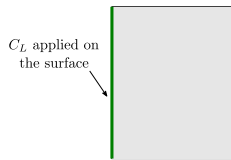
- Conduct TDS tests to identify the various trapping sites.
- Simulate desorption curves under varying conditions.



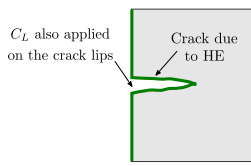
► Hydrogen boundary condition:

- Implementation of a new boundary condition that accounts for the newly created surfaces during crack propagation.

Initial boundary condition

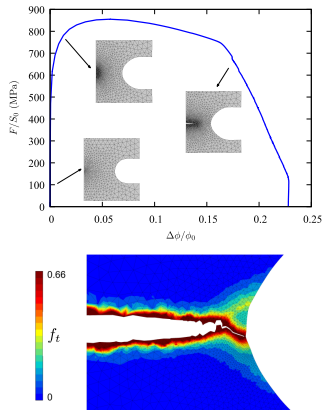


New boundary condition



► Remeshing for crack propagation:

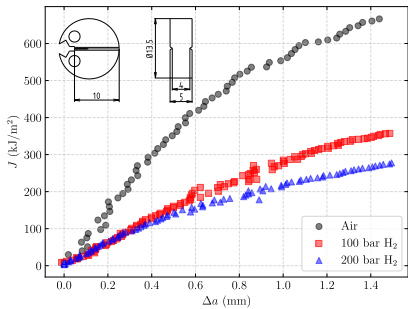
- Improve the remeshing framework to better handle 3D non-axisymmetric specimens.



(El Ouzani Tuhami *et al.*, 2022)

► Size effect & HE:

- Extend the study of hydrogen embrittlement in sub-size fracture toughness specimens.
- Analyze the interplay between size effects and hydrogen-induced damage.



(Experimental data: L. Santana)

Thank you

Daniella LOPES PINTO

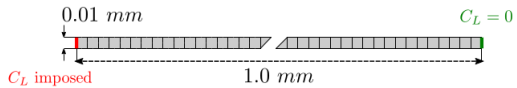
daniella.lopes_pinto@minesparis.psl.eu

Effect of traps on hydrogen diffusion

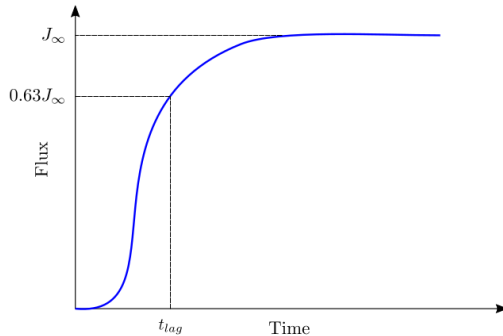
$$N_T = N_T(\varepsilon_p)$$

$$D_{lag} = \frac{\ell^2}{6t_{lag}}$$

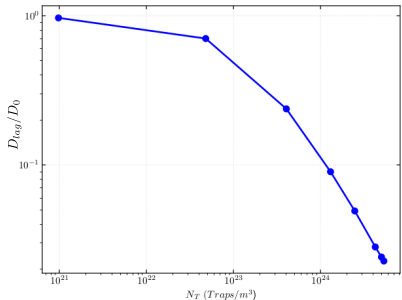
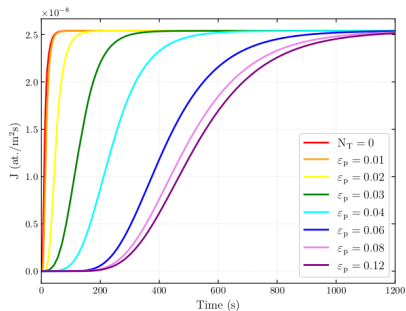
100 elements



$$W_B = 40 \text{ kJ/mol}$$



Effect of traps on hydrogen diffusion



Effect of W_B on hydrogen diffusion



$W_B = 80 \text{ kJ/mol}$



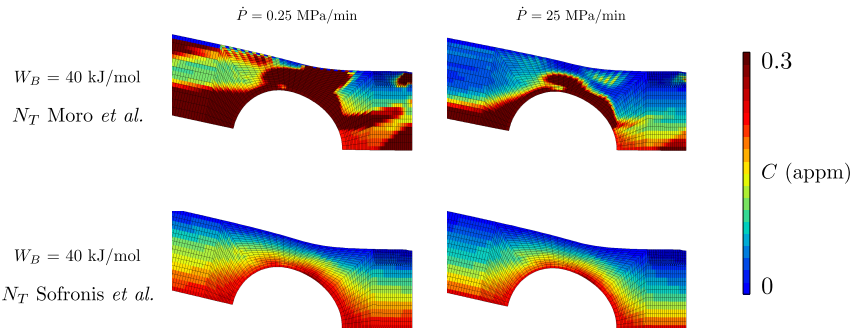
$W_B = 40 \text{ kJ/mol}$



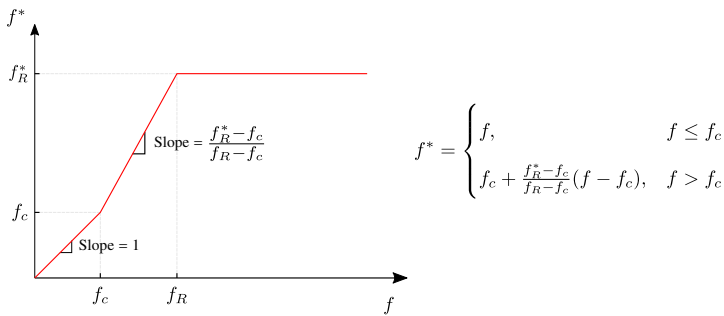
0

Concentration (appm)

2



- ▶ The introduction of the variable f_* allows for simulating the **rapid increase in porosity during the void coalescence phase**
- ▶ f_c : porosity when coalescence starts
- ▶ f_R : final porosity for ductile failure
- ▶ $f_R^* = 1/q_1$



Lattice concentration:

$$C_L = \beta N_L \theta_L$$

- ▶ β : number of NILS per solvent atom ($= 6$)
- ▶ N_L : number of solvent lattice atoms per unit lattice volume
- ▶ θ_L : occupancy of the lattice sites

Trapped concentration:

$$C_T = \alpha N_T \theta_T$$

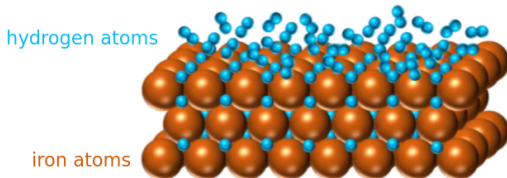
- ▶ α : number of hydrogen atom sites per trap ($= 1$)
- ▶ N_T : number of traps per unit lattice volume
- ▶ θ_T : occupancy of the trapping sites

Correction carried out by Krom *et al.* (1999):

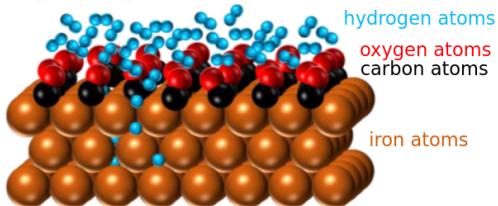
$$\frac{d}{dt} \int_V (C_L + C_T) dV + \int_S J \cdot n \, dS = 0$$

$$\frac{\partial C_T}{\partial t} = \frac{\partial C_T}{\partial C_L} \frac{\partial C_L}{\partial t} + \underbrace{\frac{\partial C_T}{\partial N_T} \frac{dN_T}{d\varepsilon_p} \frac{\partial \varepsilon_p}{\partial t}}_{\text{Added term}}$$

Hydrogen adsorption on iron surface



Carbon monoxide (CO) inhibitor of HE:

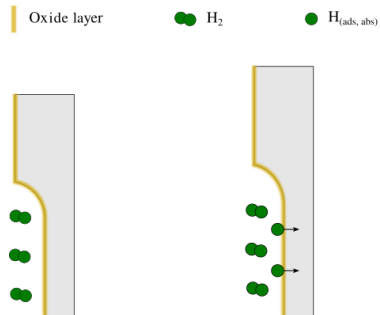


(Liu *et al.*, 2023)

- ▶ **Flux resistance:** The oxide layer on the surface creates an interfacial resistance to hydrogen penetration

$$J_n = R_H(C_L^\infty - C_L)$$

- ▶ $R_H = R_H(\kappa)$ to represent the rupture of the oxide layer



No plastic strain:

- The oxide layer is intact
- **No hydrogen penetration**

Plastic strain:

- Rupture of the oxide layer
- Hydrogen diffusion into the lattice

